WILEY-VCH

Supporting Information

Bismuth Activated Full Spectral Double Perovskite Luminescence Materials by Excitation and Valence Control for Future Intelligent LEDs Lighting

Yi Wei, [a] Hang Yang, [a] Zhiyu Gao, [a] Gongcheng Xing, [a] Maxim S. Molokeev, [b,c,d] Guogang Li *[a]

[a] *Engineering Research Center of Nano-Geomaterials of Ministry of Education, Faculty of Materials Science and Chemistry, China University of Geosciences, Wuhan, Hubei, 430074, P. R. China.*

[b] *Laboratory of Crystal Physics, Kirensky Institute of Physics, Federal Research Center KSC SB RAS, Krasnoyarsk 660036 (Russia).*

[c] *Siberian Federal University, Krasnoyarsk 660041 (Russia).*

[d] *Department of Physics, Far Eastern State Transport University, Khabarovsk, 680021 (Russia)*

Experimental Section

Materials and Preparation: A series of $La_2Mg_{(1+\delta)}Zr_{(1-\delta)}O_6$ ($0 \le \delta \le 0.14$), $La_{2(1-x)}Mg_{1.14}Zr_{0.86}O_6:xBi^{3+}$ ($0 \le x \le 0.1$) and $La_{(1.93-y)}Mg_{1.14}Zr_{0.86}O_6:0.07Bi^{3+}$, yEu^{3+} ($0 \le y \le 0.05$) samples were synthesized via a high temperature solid-state reaction in air. $La_2Mg_{(1+\delta)}Zr_{(1-\delta)}O_6$ ($0 \le \delta \le 0.14$), $La_2Mg_{1.14}A_{0.86}O_6:xBi^{3+}$ ($0 \le x \le 0.1$) and $La_{(1.93-y)}Mg_{1.14}Zr_{0.86}O_6:0.07Bi^{3+}$, yEu^{3+} ($0 \le y \le 0.05$) can be abbreviated to $LM_{(1+\delta)}Z_\delta$, $LMZ:xBi^{3+}$ and $LMZ:0.07Bi^{3+}$, yEu^{3+} respectively. In a typical preparation process, the raw materials were La_2O_3 (Aladdin), Mg_O (Aladdin), ZrO_2 (Aladdin), Bi_2O_3 (Aladdin) and Eu_2O_3 (Aladdin). All materials had a purity of ≥ 99.99% and were used without further processing. Stoichiometric raw materials were weighed, mixed together and ground sufficiently for 30 min in an agate mortar with a pestle, then the mixture was placed into alumina crucibles and sintered in a tube furnace at 1500 °C for 12 h in air. After cooling down to room temperature naturally, the resulting phosphor powders were successfully achieved after grinding again.

Characterization: The powder X-ray diffraction (XRD) data were measured on a D8 Focus diffractometer with Nifiltered Cu Kα (λ = 1.540598 Å) at a scanning rate of 1° min^{-1} in the 2θ range from 5° to 100°. Rietveld refinements based on XRD data were performed on General Structure Analysis System (GSAS) software. X-ray photoelectronic spectroscopy (XPS) spectra were performed on Thermo ESCALAB 250XI. The morphologies were performed by using a field emission scanning electron microscope (FE-SEM, S-4800, Hitachi). The diffuse reflectance (DR) spectra were measured on UV−visible diffuse reflectance spectroscopy (UV-2550PC, Shimadzu Corporation, Japan). The photoluminescence excitation (PLE) and emission (PL) spectra were obtained by using a Fluoromax-4P fluorescence spectrometer over the wavelength range 200-650 nm (Horiba Jobin Yvon, New Jersey, U.S.A.) equipped with a 150 W xenon lamp as the excitation source, and both excitation and emission spectra were set up to be 1.0 nm with the width of the monochromator slits adjusted to 0.50 nm. The photoluminescence decay curves were analyzed on a Lecroy Wave Runner 6100 Digital Osilloscope (1 GHz) using a tunable laser (pulse width = 4 ns; gate = 50 ns) as the excitation (Contimuum Sunlite OPO).

Results and discussion

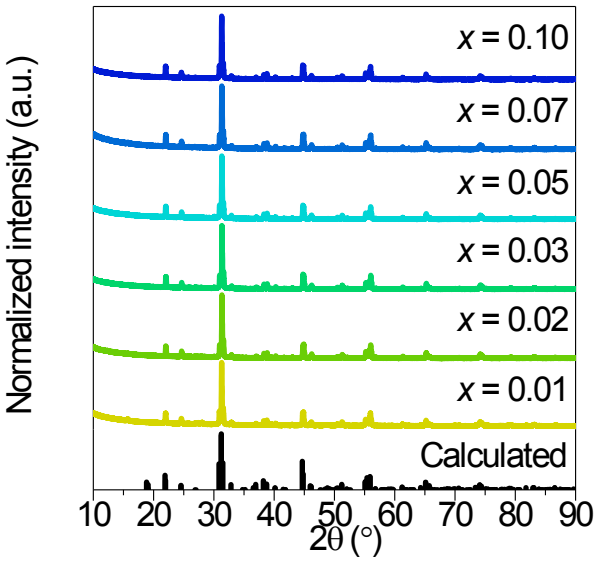

Fig. S1 XRD patterns of LMZ:xBi^{3+} ($0.01 \leq x \leq 0.1$) samples and the calculated XRD data of LMZ matrix.

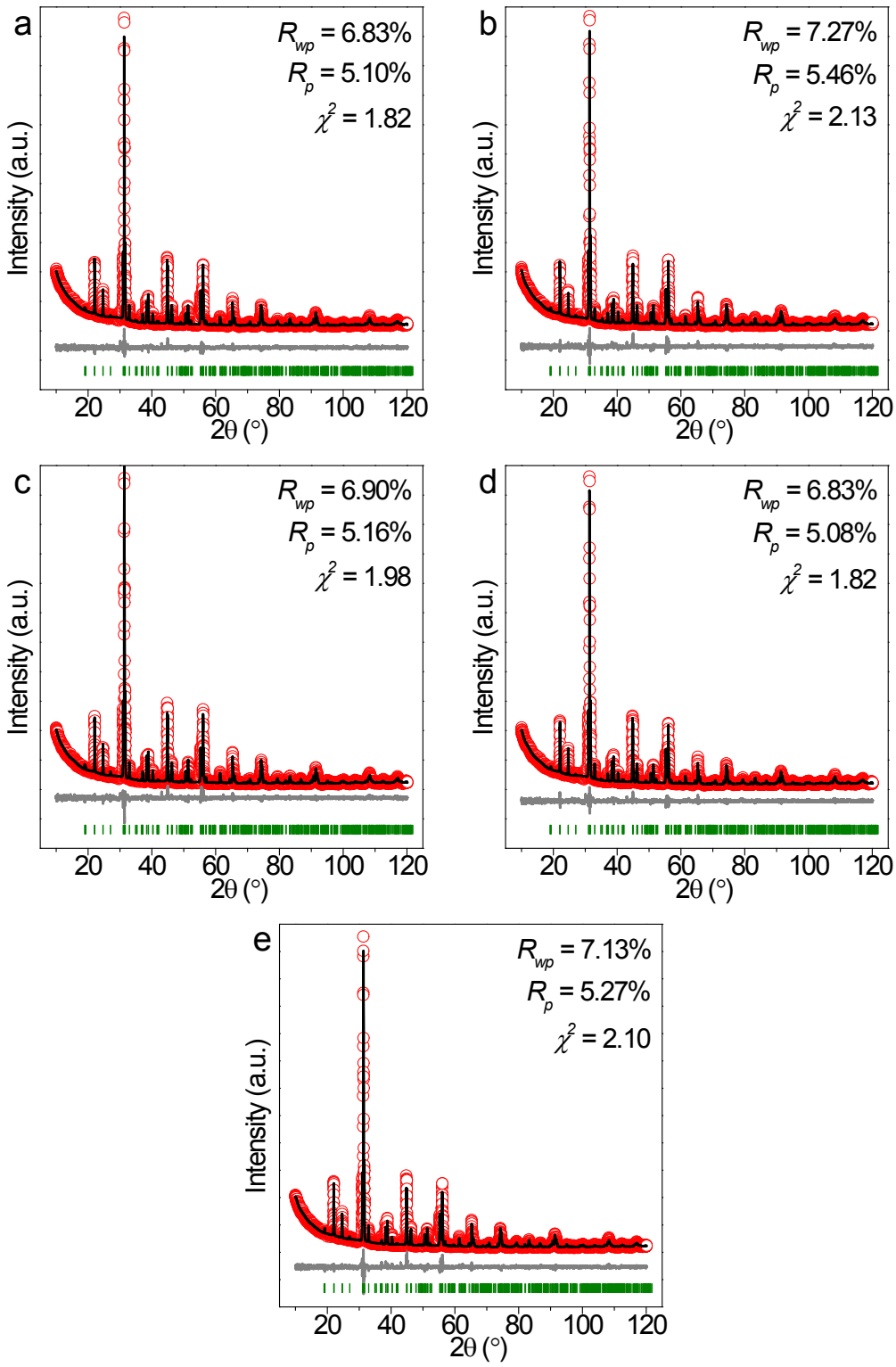

Fig. S2 Rietveld refinement data of (a) LMZ:0.01Bi^{3+}, (b) LMZ:0.02Bi^{3+}, (c) LMZ:0.03Bi^{3+}, (d) LMZ:0.05Bi^{3+} and (e) LMZ:0.10Bi^{3+} samples with the measured data (red circle), fitted data (black line), difference (grey line) and Bragg positions (olive vertical bar).

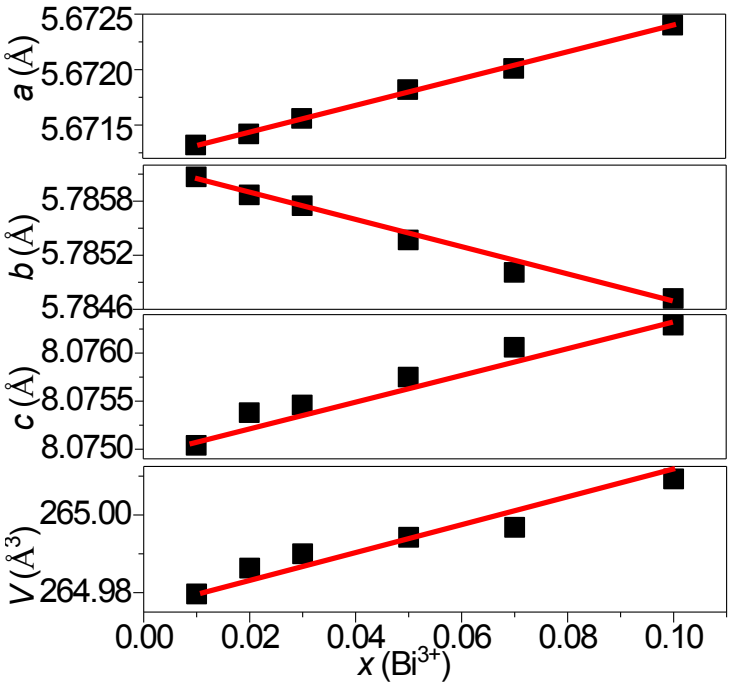

Fig. S3 The unit cell parameters of LMZ:0.07Bi^{3+} (*a*, *b*, *c* and *V*) as a function of Bi^{3+} concentrations (x).

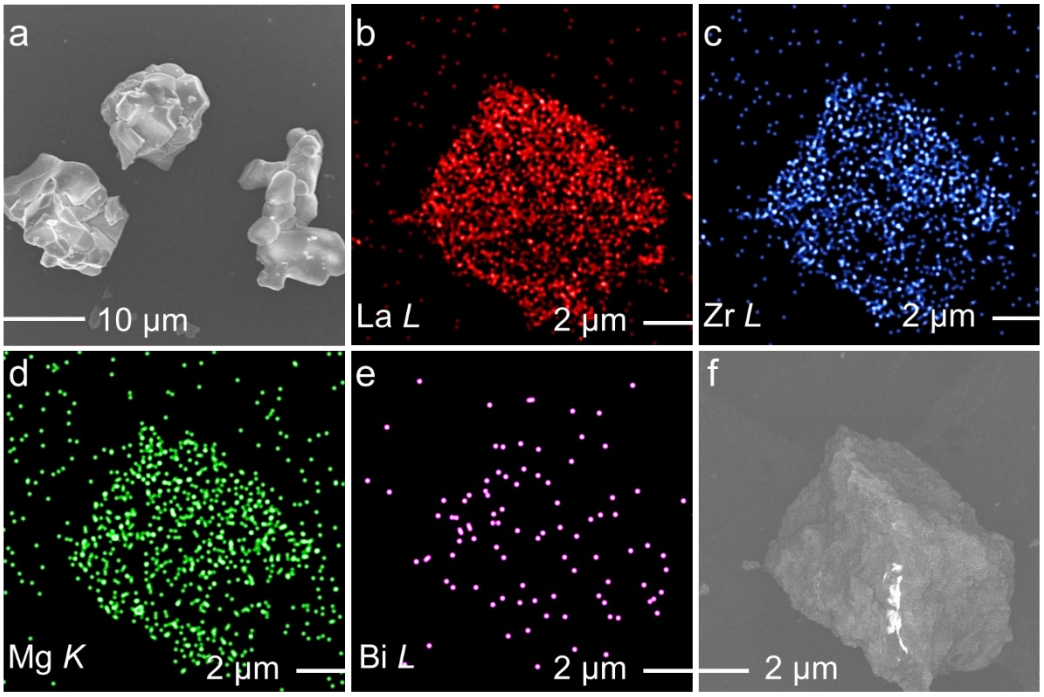

Fig. S4 (a-e) The corresponding elemental mapping analysis for La, Zr, Mg, and Bi elements in LMZ:0.07Bi^{3+}. (f) The SEM image of LMZ:0.07Bi^{3+}.

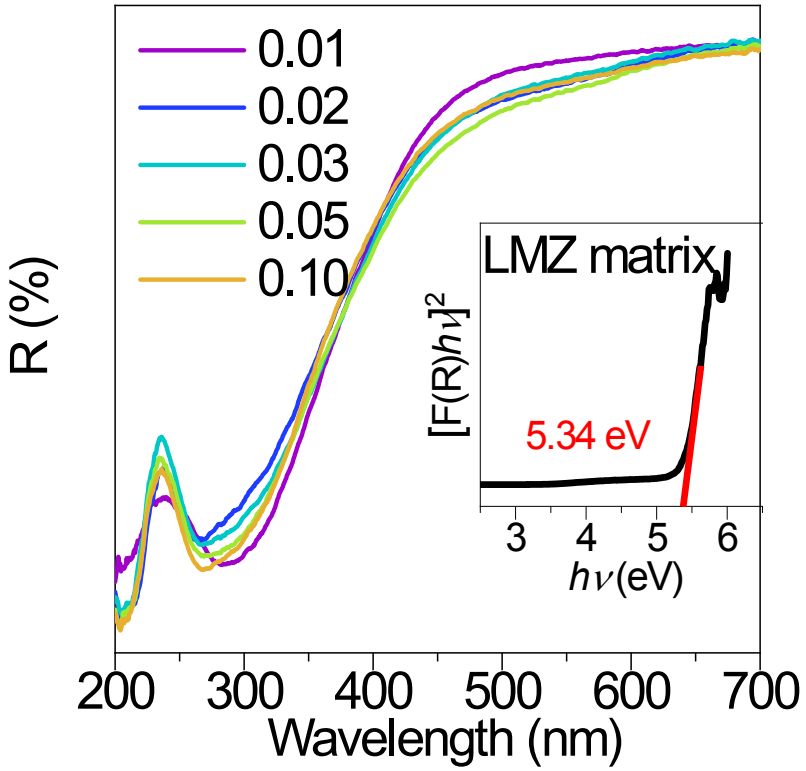

Fig. S5 DR spectra of LMZ:xBi^{3+} (0.01≤x ≤ 0.10) samples.

The direct bandgap of LMZ matrix is calculated by following formula:

$[F(R)hv]^2 = A\ (hv-E_g)$, $F(R) = (1-R)^2/2R$ (1)

Where A stands for absorption constant, E_g represents the optical bandgap, hv is the photon energy, F(R) is the absorption coefficient, and R is the reflectance (%) coefficient, respectively.

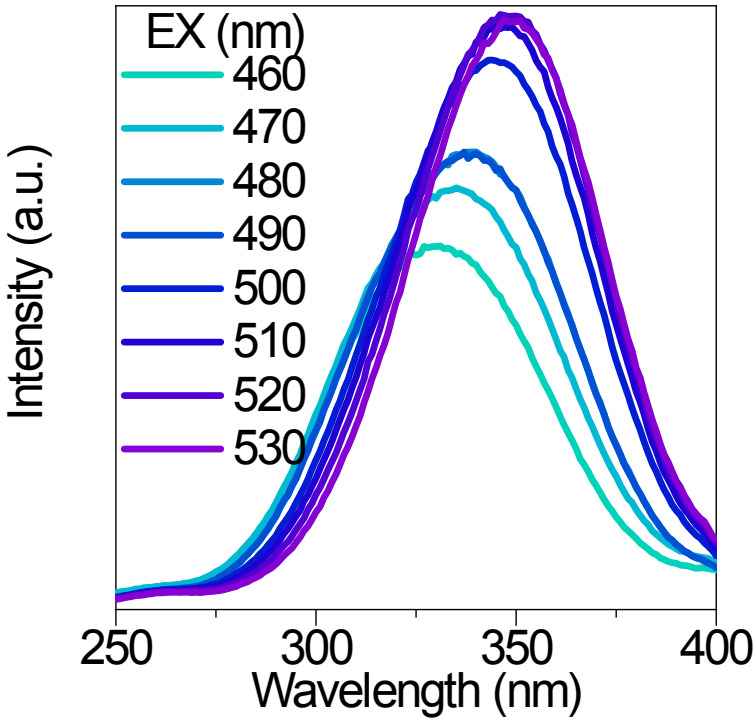

Fig. S6 The PLE spectra of LMZ:0.07Bi^{3+} (λ_{em} = 460-530 nm).

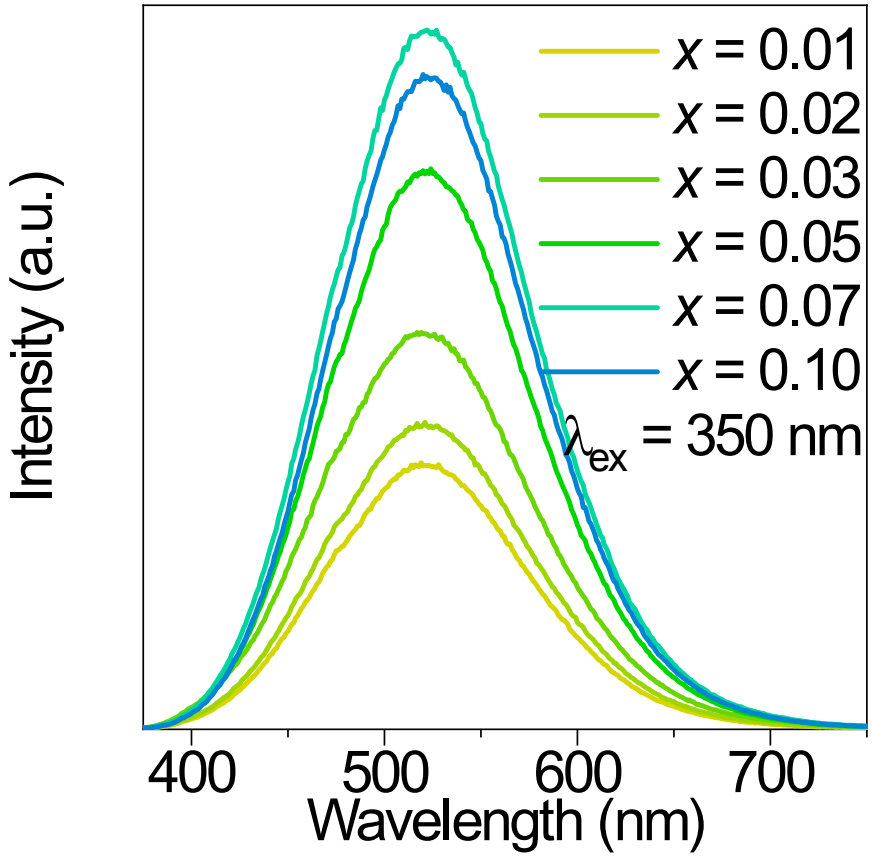

Fig. S7 The PL spectra of LMZ:xBi^{3+} (λ_{ex} = 350 nm).

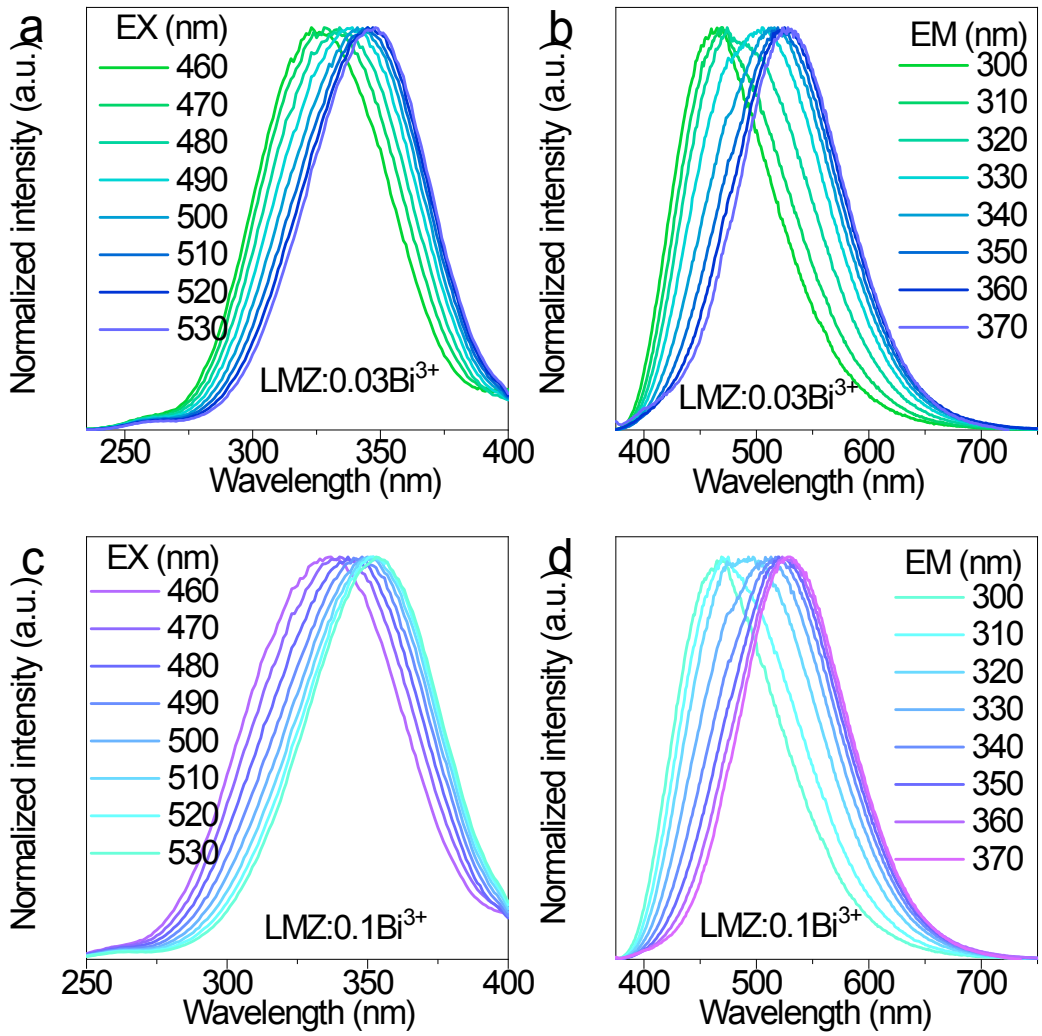

Fig. S8 Normalized PLE and PL spectra of (a-b) LMZ:0.03Bi^{3+} and (c-d) LMZ:0.1Bi^{3+}, respectively.

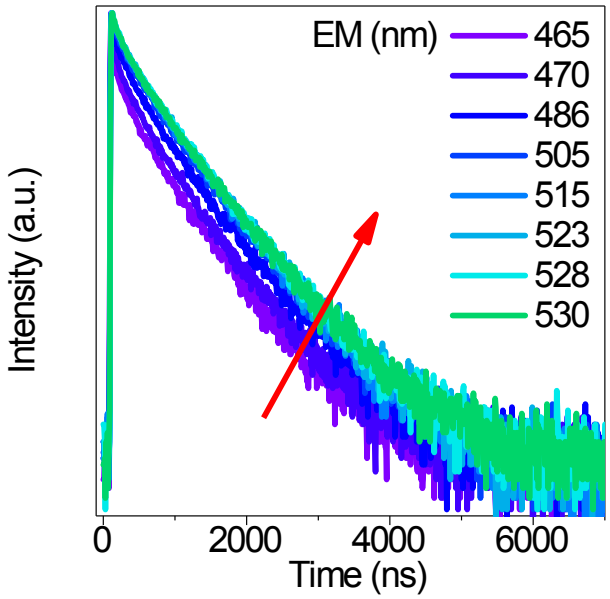

Fig. S9 Photoluminescence decay curves of LMZ:0.07Bi^{3+} (λ_{ex} = 375 nm, λ_{em} = 465-530 nm).

$$I=A_1\exp(-\tau/t_1)+I_0 \quad (2)$$

where I_0 and I_t represent luminescence intensities of Bi^{3+} at t_0 and t; τ stands for luminescence decay lifetimes for corresponding samples. A_1 is a constant.

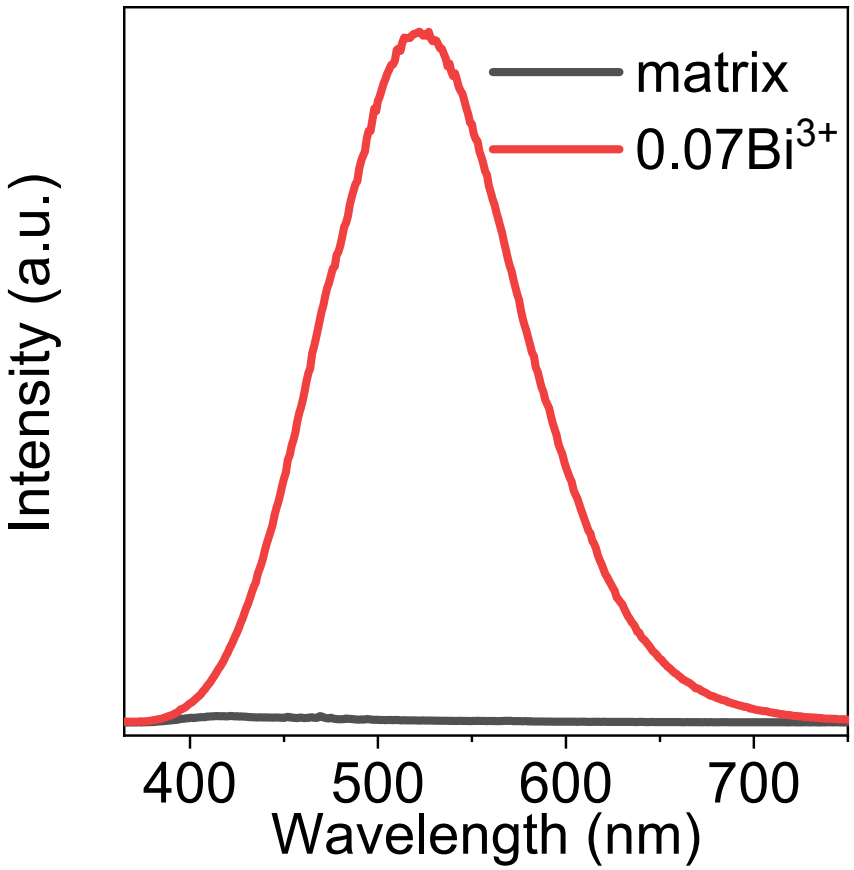

Fig. S10 The PL spectra of LMZ matrix and LMZ:0.07Bi^{3+} (λ_{ex} = 350 nm).

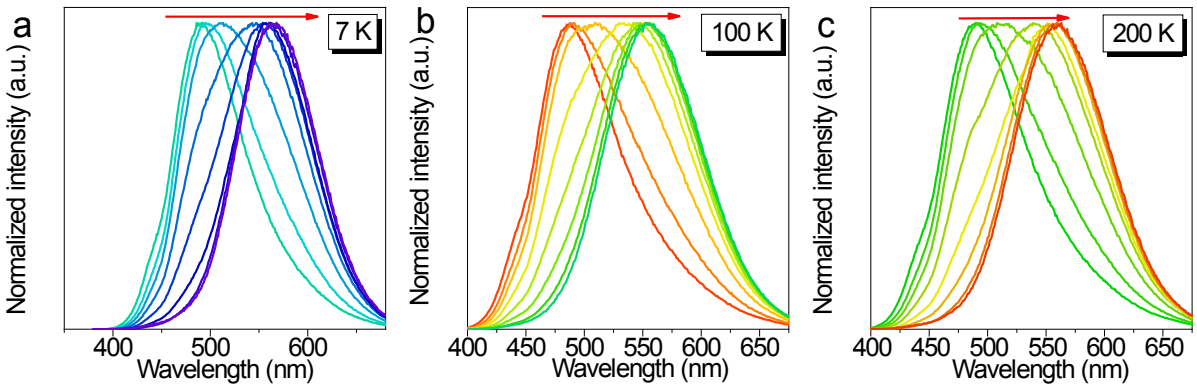

Fig. S11 Low-temperature (7, 100 and 200 K) spectra of LMZ:0.07Bi^{3+} with varying excitation and emission wavelength, respectively.

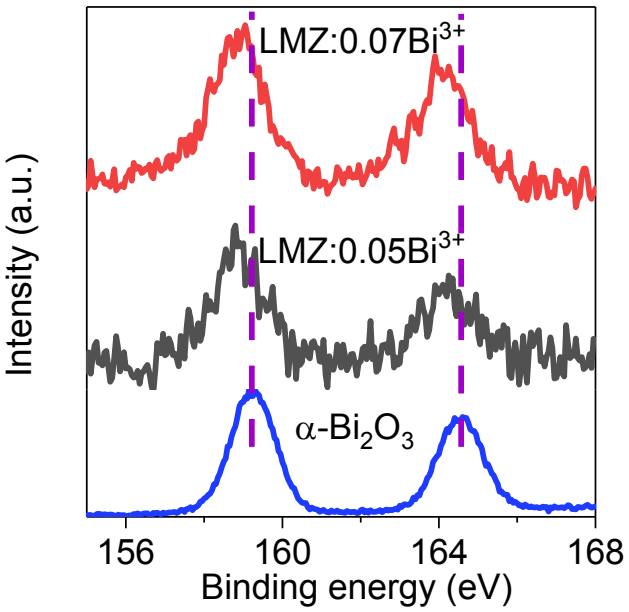

Fig. S12 XPS spectra of Bi 4f for α-Bi_2O_3, LMZ:0.05Bi^{3+} and LMZ:0.07Bi^{3+}, respectively.

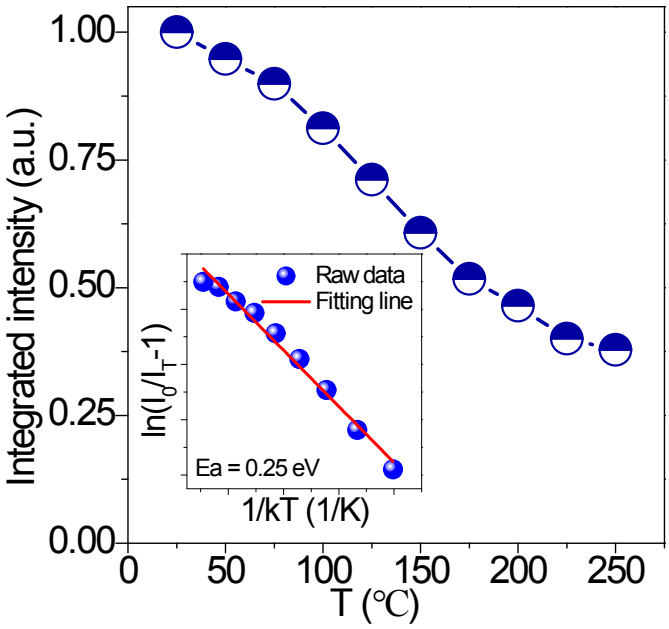

Fig. S13 Temperature-dependent integrated PL spectra of LMZ:0.07Bi^{3+}. The inset is dependence of $\ln(I_0/I_T-1)$ on 1/kT for LMZ:0.07Bi^{3+} phosphor.

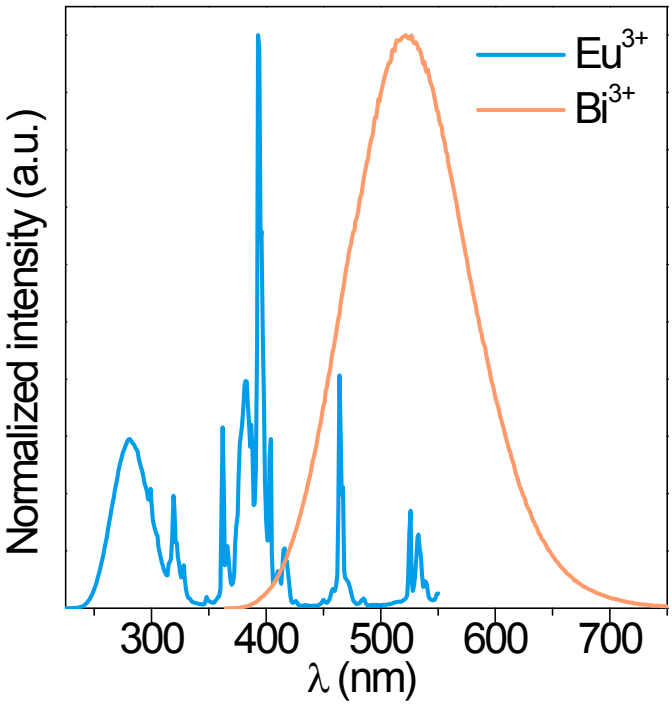

Fig. S14 PLE spectra of LMZ:0.05Eu^{3+} and PL spectra of LMZ:0.07Bi^{3+} (λ_{ex} = 350 nm).

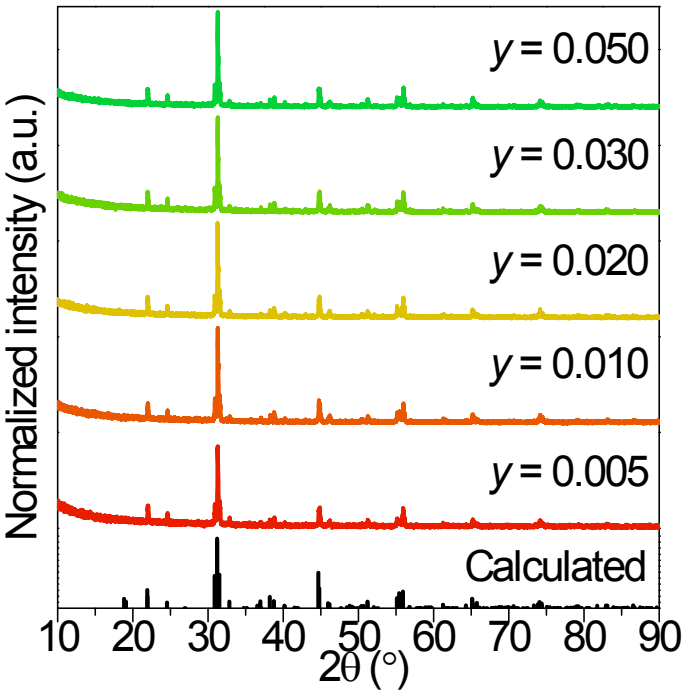

Fig. S15 XRD patterns of LMZ:0.07Bi^{3+}, yEu^{3+} (0 ≤ y ≤ 0.05) samples and the calculated data of LMZ.

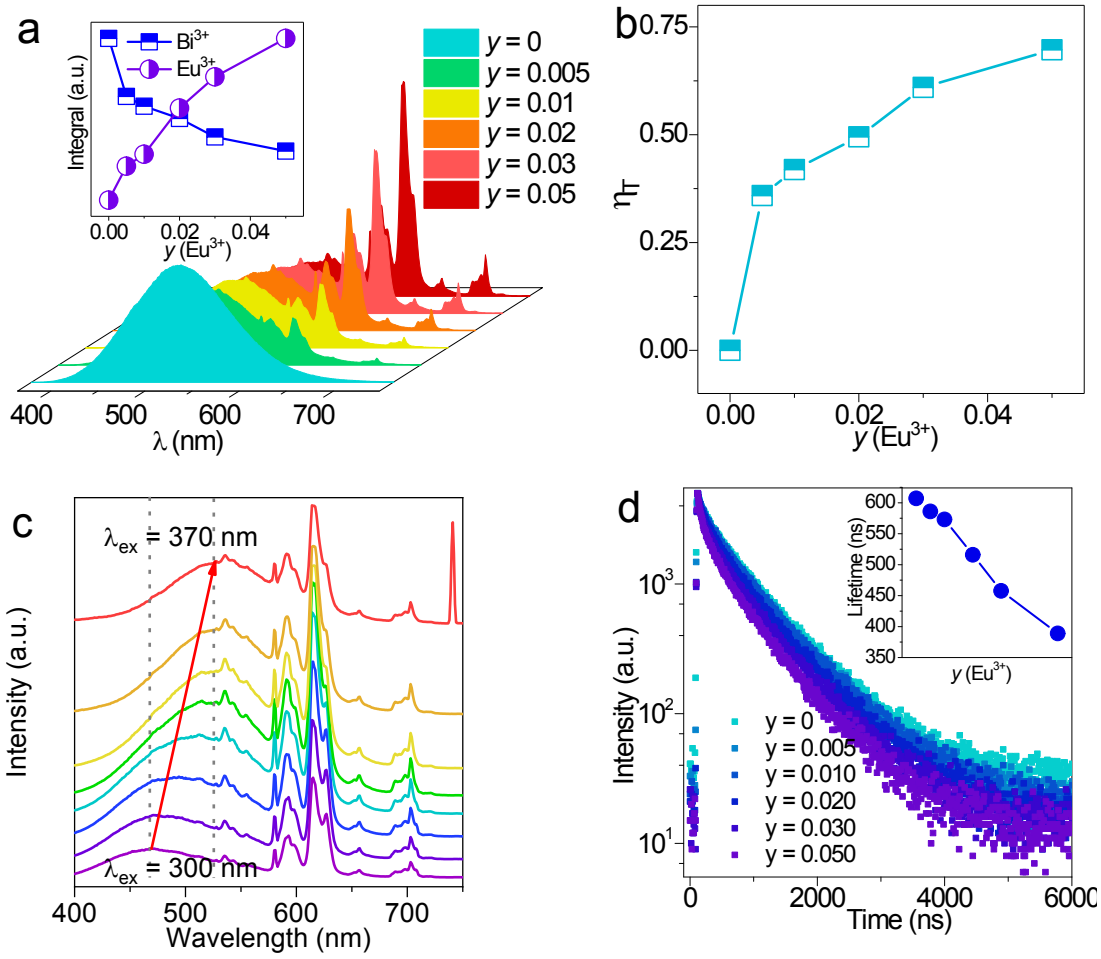

Fig. S16 (a) PL spectra of LMZ:0.07Bi^{3+}, yEu^{3+} (0 ≤ y ≤ 0.05) excited at 350 nm, and the inset is integrated intensity of Bi^{3+} and Eu^{3+} as a function of Eu^{3+} concentrations. (b) Energy transfer efficiency of LMZ:0.07Bi^{3+}, yEu^{3+} (0 ≤ y ≤ 0.05). (c) PL spectra of LMZ:0.07Bi^{3+}, 0.02Eu^{3+} under various excitation wavelength (300-370 nm). (d) Photoluminescence decay curves of LMZ:0.07Bi^{3+}, yEu^{3+} (0 ≤ y ≤ 0.05) detected at 350 nm.

The energy transfer efficiency is calculated by the following equation:

$$\eta_T = 1 - \frac{I_S}{I_{S0}} \qquad (3)$$

where η_T stands for the energy transfer efficiency, I_S and I_{S0} represent emission intensity with and without Eu^{3+} ions respectively. The energy transfer efficiency of LMZ:0.07Bi^{3+}, yEu^{3+} are 0.36, 0.42, 0.50, 0.61 and 0.70, respectively (Fig. S16b), which mean effective energy transfer happening in LMZ:0.07Bi^{3+}, yEu^{3+}.

Under 350 nm n-UV light exciting, the photoluminescence decay lifetime for Bi^{3+} emission of LMZ:0.07Bi^{3+}, yEu^{3+} samples are determined via the equation (2). With the increase of Eu^{3+} concentrations (y), the decay lifetimes are calculated to be 607, 586, 573, 516, 458, and 389 ns for y = 0, 0.01, 0.02, 0.03, 0.04, 0.05, respectively. The above results are shown in Fig. S16d.

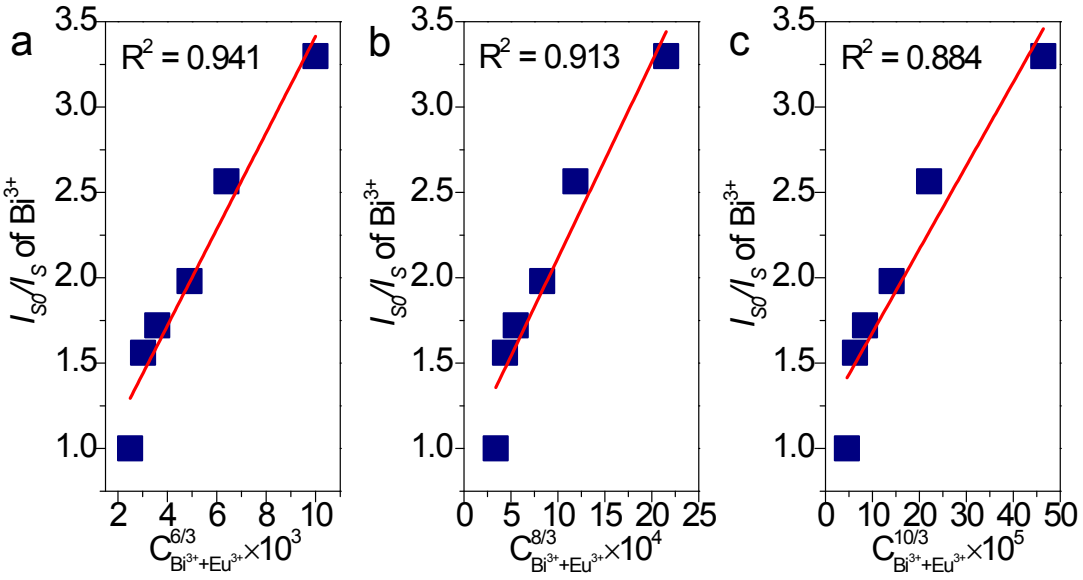

Fig. S17 Dependence of I_{S0}/I_S of Bi^{3+} ions on (a) $C^{6/3}_{(Bi^{3+}+Eu^{3+})}$, (b) $C^{8/3}_{(Bi^{3+}+Eu^{3+})}$ and (c) $C^{10/3}_{(Bi^{3+}+Eu^{3+})}$ for LMZ:0.07Bi^{3+}, yEu^{3+} ($0 \le y \le 0.05$).

$$R_c \approx 2\left(\frac{3V}{4\pi x_c N}\right)^{1/3} \quad (4)$$

Where V is the volume of the unit cell, x_c is the sum concentration of Bi^{3+} ions and Eu^{3+} ions, N is the number of cations in the unit cell.

$$\frac{\eta_{S0}}{\eta_S} \propto C^{n/3} \quad (5)$$

Where η_{S0}/η_S stands for the ratio of quantum efficiency without and with Bi^{3+}-doped samples. C represents the total concentration of Bi^{3+} and Eu^{3+} ions. n is a constant which influences the interaction relationship of Bi^{3+} and Eu^{3+}, when *n* = 6, 8, and 10, matching with dipole–dipole, dipole–quadrupole and quadrupole–quadrupole interactions, respectively. The value of η_{S0}/η_S could be approximately replaced by the ratio of emission intensity of I_{S0}/I_S. Hence, the formula can be expressed as follow:

$$\frac{I_{S0}}{I_S} \propto C^{n/3} \quad (6)$$

where I_{S0} represents initial emission intensity of Bi^{3+}, and I_S represents emission intensity Bi^{3+} of Bi^{3+}/Eu^{3+} co-doped phosphors. According to the results, dipole–dipole dominate concentration quenching effect in LMZ:0.07Bi^{3+}, yEu^{3+}.

Table S1. Main parameters of processing and refinement of the LMZ:0.07Bi^{3+} samples.

Space group	*P21/n*
Unit cell	*a* = 5.67758(9)
Unit cell	*b* = 5.79067(9)
Cell volume	*c* = 8.0838(1)
	V = 265.770(7)
R_{wp}	6.39%
R_p	4.82%
χ^2	1.23

Table S2. Fractional atomic coordinates and isotropic displacement parameters (Å^2) of LMZ:0.07Bi^{3+}.

	x	y	z	B_{iso}	Occ.
La	0.5084 (5)	0.54261 (17)	0.2537 (7)	0.30 (10)	1
Mg1	0.5	0	0	0.3 (5)	0.401 (35)
Zr1	0.5	0	0	0.3 (5)	0.599 (35)
Mg2	0	0.5	0	0.3 (5)	0.507 (34)
Zr2	0	0.5	0	0.3 (5)	0.493 (34)
O1	0.210 (14)	0.209 (9)	-0.051 (6)	0.5 (2)	1
O2	0.293 (14)	0.688 (8)	-0.059 (7)	0.5 (2)	1
O3	0.417 (2)	-0.0244 (19)	0.251 (11)	0.5 (2)	1

Table S3. The calculated value of PL decay curves of LMZ:0.07Bi^{3+} emission detected at 375 nm with different emission wavelength (465-530 nm).

Monitored wavelength (nm)	Lifetime (ns)
465	448.8
470	477.1
486	535.3
505	585.8
515	598.5
523	607.9
528	608.2
530	613.0

Table S4. CIE color coordinates of LMZ:0.07Bi^{3+}, yEu^{3+} (0 ≤ y ≤ 0.05) with varying excitation wavelength.

Samples	CIE x	CIE y	Excitation wavelength
y = 0	0.1828	0.2361	300
	0.1985	0.2803	310
	0.2202	0.3304	320
	0.2427	0.3773	330
	0.2628	0.4159	340
	0.2802	0.4473	350
	0.2949	0.4712	360
	0.3062	0.4867	370
y = 0.01	0.2324	0.2539	300
	0.2398	0.2904	310
	0.2555	0.3353	320
	0.2735	0.3791	330
	0.2905	0.4154	340
	0.3053	0.4432	350
	0.3178	0.4634	360
	0.3256	0.4725	370
y = 0.02	0.2757	0.2716	300
	0.2772	0.3033	310
	0.287	0.3434	320
	0.2997	0.3833	330
	0.3128	0.4165	340
	0.3249	0.4421	350
	0.3355	0.4604	360
	0.3422	0.4692	370
y = 0.03	0.3717	0.3023	300
	0.3657	0.325	310
	0.3656	0.3552	320
	0.3671	0.3862	330
	0.3713	0.4129	340
	0.3771	0.4333	350
	0.3827	0.4475	360
	0.3855	0.4534	370
y = 0.05	0.5075	0.332	300
	0.5017	0.3441	310
	0.4931	0.3604	320
	0.4828	0.3785	330
	0.4755	0.395	340
	0.4718	0.4077	350
	0.471	0.4158	360
	0.4692	0.4185	370